



Preparation and characterization of γ -alumina ceramic ultrafiltration membranes for pretreatment of oily wastewater

Arash Bayat, Hamid Reza Mahdavi, Mansour Kazemimoghaddam, Toraj Mohammadi*

Research and Technology Centre for Membrane Processes, Faculty of Chemical Engineering, Iran University of Science and Technology (IUST), Narmak, Tehran, Iran, Tel./Fax: +98 21 77240051; emails: bayaat.iust@gmail.com (A. Bayat), hamidreza_mahdavi@chemeng.iust.ac.ir (H.R. Mahdavi), mzkazemi@yahoo.com (M. Kazemimoghaddam), torajmohammadi@iust.ac.ir (T. Mohammadi)

Received 2 September 2015; Accepted 5 January 2016

ABSTRACT

The main goal of the present study is to prepare γ -alumina (γ - Al_2O_3) ultrafiltration (UF) membranes for separation of oil from a real oily wastewater. A γ - Al_2O_3 multilayer UF membrane on an α -alumina (α - Al_2O_3) substrate was successfully fabricated via the sol-gel processing method. The prepared layer from the γ - Al_2O_3 colloidal sol as the membrane top layer had an average pore size of 20.3 nm and thickness of 4 μm . The resulting γ - Al_2O_3 multilayer UF membrane did exhibit homogeneity with no cracks or pinholes. Permeate flux (PF) through the membranes was calculated. Response surface methodology (RSM) based on Box-Behnken design was used to design the experiments and analyze three operating parameters including transmembrane pressure (TMP), feed temperature (T), and cross-flow velocity (CFV). The optimum PF of 112.7 $\text{kg}/\text{m}^2 \text{h}$ was identified by RSM at feed temperature of 35 $^\circ\text{C}$, TMP of 5 bar and CFV of 0.735 m/s . The results showed that these membranes are efficient for treatment of petroleum refinery wastewater, so that total suspended solids, chemical oxygen demand, biological oxygen demand, total organic carbon, oil and grease content, turbidity, and pH are reduced by 86, 73, 63, 67, 84, 79, and 7%, respectively. The prepared γ - Al_2O_3 UF membranes exhibited great potential to be employed as an advanced method for pretreatment of oily wastewater due to its ability for physical separation of contaminants and commercial aspects.

Keywords: Oily wastewater treatment; Ultrafiltration; Inorganic ceramic membrane

1. Introduction

Every year, large volume of oily wastewater is produced and this results in horrible environmental pollution and resource usage problems. Conventional oily wastewater treatment methods, including gravity separation and skimming, coagulation, air flotation, flocculation and de-emulsification, have their intrinsic

disadvantages such as low efficiency, high operation cost, corrosion, and decontamination difficulties [1,2]. Also, conventional biological and/or chemical methods are very difficult because of their high oil and grease content (OGC) and total suspended solids (TSS) and chemical oxygen demand (COD) concentrations. A suitable treatment method needs to continuously reduce all these pollutants of the wastewater to acceptable levels to discharge the treated wastewater

*Corresponding author.

for reuse. During the last 20 years, oily wastewater treatment by membranes has been widely studied. Different issues like effects of pH [3,4], temperature (T), presence of organic compounds [5], pretreatment [6], fouling [7], foulant composition [8,9], coagulant addition [10], salt concentration [11], emulsion stability [12], filtration equipment type: cross-flow, dead-end and rotational disk [13], cleaning [14], membrane materials [13,15], and also modeling of fouling and flux decline by empirical or theoretical models [16,17] have been investigated.

Lately, several types of pressure-driven membrane processes such as microfiltration (MF), ultrafiltration (UF), nanofiltration (NF), and reverse osmosis (RO) have been applied for oil/water emulsions separation [18–21]. Because of its appropriate pore size (usually in the range of 2–50 nm) and capability of removing emulsified oil droplets without any de-emulsification process, UF has been introduced as an efficient method or a pretreatment step before NF and RO in oil/water emulsions treatment [22].

UF membranes are mainly classified into two types of polymeric and inorganic membranes. Inorganic membranes are completely appropriate for processes involving thermal stability, good chemical stability, mechanical resistance, pressure resistance, long life, and good antifouling properties, and have been successfully utilized for refinery wastewater treatment. Nowadays, ceramic UF membranes are being widely applied to treat oil/water emulsions. It is because of their distinct advantages like chemical inertness, temperature, and damage resistance and well-defined stable pore structure [23,24]. Ceramic membranes could be made from alumina, mullite, cordierite, silica, spinel, zirconia, and other refractory oxides [25,26]. Among them, alumina ceramic membranes have very high chemical and thermal stability. Applications of alumina membranes have been little discussed in literature [11,27,28]. Therefore, it was decided to synthesize these potentially commercial membranes and investigate their performance for treatment of a real oily wastewater. The major drawback in employing them is the inherent fouling phenomena found in all membrane systems. During operation, membrane fouling causes a progressive decrease in flux and induces a loss of separation efficiency. Based on the separation process and the type of membrane used, different cleaning strategies can be employed [14,29,30].

In this research, a cheap γ -alumina (γ - Al_2O_3) membrane (using locally available materials) was prepared. A thin top layer (γ - Al_2O_3) was fabricated using boehmite sol via dip-coating technique on an α -alumina (α - Al_2O_3) support. Characteristics of γ - Al_2O_3 were investigated by means of XRD analysis. Then,

effects of temperature, transmembrane pressure (TMP), and cross-flow velocity (CFV) on UF of oily wastewater represented by permeate flux (PF) of the membrane during treatment of the real oily wastewater were investigated. Also, at the best operating condition, performance of the γ - Al_2O_3 membrane during treatment of the real oily wastewater was studied.

2. Materials

In this study, commercial grade of α - Al_2O_3 with 99.6% purity with average particle size of 1 μm , carboxymethyl cellulose (CMC, Merck) as polymeric binder, and double-distilled water for support preparation were used. To obtain a porous metal oxide film via hydrolysis of an alkoxide, a stable nanoparticles suspension of the metal oxide was prepared. Aluminum tri-sec-butoxide (ATSB, Merck) as alkoxide precursor, nitric acid (HNO_3 , Merck) as peptization agent, polyvinyl alcohol (PVA, Merck) with an average molecular weight of 145 kDa were as drying chemical-controlling additive and deionized water were used for production of the metal oxide sol.

3. Experimental setup

In order to carry out the experiments almost close to an industrial scale, an experimental setup as shown in Fig. 1 was designed and fabricated. The membrane surface area in contact with the feed was equal to 315 mm^2 . It was simple and had no complexity; however, it was designed in such a way that all important operating parameters in the UF process could be tuned and controlled. The system was operated in a cross-flow mode. Consequently, the feed stream did flow on the membrane surface in a parallel direction and only a small part of the feed was processed by the membrane. In all cases of practical applications of UF, all or part of the processed feed is recycled. This form was selected to avoid concentration polarization

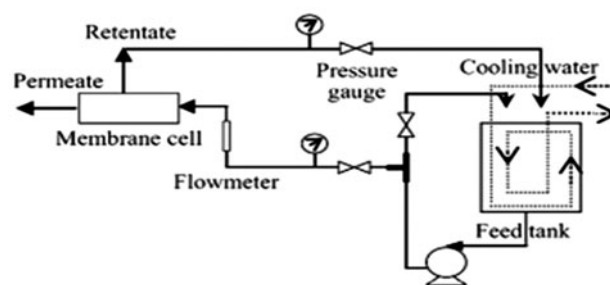


Fig. 1. Experimental setup.

and membrane fouling. The system mentioned above consisted of a vessel with a capacity of 10 L with a tubular heat exchanger in order to control the feed temperature and also a stirrer in order to keep the feed uniform. The feed temperature was controlled by a digital thermometer with an accuracy of $\pm 0.1^\circ\text{C}$.

4. Experimental procedure

The membrane permeate was collected in an Erlenmeyer and measured using a digital balance with an accuracy of ± 0.1 g. During the experiments, exact supervision was performed on controllable factors (T , CFV, and TMP) and industrial reservations were considered. To study the effect of T , CFV, and TMP on the PF, they were varied from 25 to 45°C , 0.59 to 0.88 m/s, and 2 to 5 bar, respectively. Also operation time for the membrane filtration was 90 min. All of the measurements and adjustments for the UF membrane experiments were the same. It must be mentioned that for each experiment a new membrane was used to have the same experimental conditions for all the experiments. PF was calculated as follows:

$$\text{PF} = \frac{M}{At} \quad (1)$$

where M is mass of permeate collected per unit effective membrane area (A) per unit time (t).

5. Membrane preparation

As top layer, $\gamma\text{-Al}_2\text{O}_3$ was synthesized over mesoporous $\alpha\text{-Al}_2\text{O}_3$ support (disk-shaped, diameter 21 mm, thickness 1.8 mm, porosity 45%) surface to improve the membrane performance. The method developed by Yoldas [31] was used for making clear Al_2O_3 sol. Stable boehmite sol of 1 M aluminum concentration was prepared from hydrolysis and condensation of ATSB. Then, alkoxide precursor was slowly hydrolyzed in water at $80\text{--}85^\circ\text{C}$, and after 1 h of stirring, the resulting slurry with AlOOH precipitates was peptized with nitric acid at $\text{HNO}_3/\text{AlOOH}$ molar ratio of 0.07. This step prevented agglomeration of the sol particles and destructed very large agglomerates to form highly dispersed, stable colloidal solution. The peptization process was carried out for 2 h at 90°C in an uncovered reaction flask in order to allow the remaining alcohol to evaporate. Then, it was continued by refluxing under continuous stirring at $90\text{--}100^\circ\text{C}$ for 12 h in order to ensure complete mixing and hydrolysis and colloidal formation.

Aqueous PVA solution was then added to the solution of the resulted sol to prevent crack formation in the membrane structure during drying process. The content of organic molecules for each 30 ml of the sol was 20 ml of the aqueous PVA solution at a concentration of 3 g per 100 cm^3 . For preparation of a uniform layer, the substrate was coated with the Al_2O_3 colloidal solution via dip-coating method. In this procedure, the substrate was immersed in fresh boehmite/PVA mixture for 5 s. The supports were removed from the dipping sol and the excess sol was dried. The samples were dried at 40°C for 2 d and then calcined at 550°C for 3 h at 1°C min^{-1} heating rate. In order to suppress eventual pinholes and small defects, the coating, such an operation as mentioned previously, was repeated to obtain a crack-free film.

6. Membrane characterization

Milk concentration is typically used for characterization of UF membranes. The experiments were carried out at temperature of 25°C and pressure of 3 bar for each time of coating. In order to foul the membrane, milk with 2.5% fat was mixed with water in proportion of 70% milk and 30% water and used as the feed.

XRD measurements were conducted by a Siemens diffractometer using Cu K radiation working at 30 mA and 40 kV. The SEM images were obtained using a Vega Tescan scanning electron microscope. BET characterization of the active layer at adsorption temperature of 77 K and vapor pressure of 88.7 kPa. Also XRD measurement, SEM image, and BET analysis were performed for determining $\gamma\text{-Al}_2\text{O}_3$ phase, coating uniformity and adhesiveness to support, and average pore size and specific surface area of $\gamma\text{-Al}_2\text{O}_3$, respectively.

7. Process feed

Outlet of the API separator unit of Shahid Dolati's separation pool in Karaj, Iran was used as feed. The feed was taken weekly and used immediately. Analysis of the feed as an oily wastewater is presented in Table 1. Original temperature of the feed was in the range of $25\text{--}30^\circ\text{C}$ depending on the season.

7.1. Analysis of samples

Samples for measurements of the feed and the permeate TSS, biological oxygen demand (BOD_5), COD, total organic carbon (TOC), OGC, and turbidity were taken as necessary and analyzed via the procedure

Table 1
Characteristics of the process feed and permeate

Parameter	Unit	Feed	Permeate	Rejection (%)
TSS	mg/l	210	30	86
COD	mg/l	456	125	73
BOD5	mg/l	237	86	63
TOC	mg/l	215	72	67
OGC	mg/l	69	11	84
Turbidity	NTU	173	37	79
pH	–	8	7	–

Note: Rejection was determined under TMP of 5 bar and CFV of 0.735 m/s.

outlined in standard methods [32]. Turbidity was estimated using Turbidimeter (Hach Model 2100A Turbidimeter, United States).

8. Experimental design

The process variables of UF for oily wastewater treatment were investigated and optimized using response surface methodology (RSM). It was utilized to design the experiments, and optimize PF as response value. The number of experiments was optimized by Box–Behnken design (BBD) in order to verify the interactions between the major operating variables and their influences on PF. According to previous studies [3,6,28,33,34], three parameters were selected. It was believed that they have the greatest effect on UF process. As shown in Table 2, the three parameters were adjusted each with three levels (low, medium, and high appointed as –1, 0, and 1, respectively). Consequently, the number of experiments required to investigate the parameters at three levels was 15. The center point in the design was repeated three times for estimation of errors and curvature. The results from this limited number of experiments proposed a statistical model. The statistical design and data analysis were accomplished by Design-Expert 7.0.0 software. Experimental points for BBD are shown in Table 3.

The regression analysis was performed to estimate the response function predicted by the quadratic model as shown in Eq. (2):

Table 3
BBD for the membrane process based on the uncoded values

Run	T (°C)	P (bar)	CFV (m/s)	PF (kg/m ² h)
1	45	3.5	0.59	103.5
2	35	3.5	0.735	107.9
3	25	3.5	0.88	86.8
4	35	3.5	0.735	108.1
5	35	5	0.59	111.0
6	45	2	0.735	75.0
7	25	3.5	0.59	94.2
8	35	3.5	0.735	107.0
9	35	2	0.59	74.5
10	35	2	0.88	67.1
11	25	5	0.735	102.2
12	25	2	0.735	65.7
13	45	5	0.735	111.5
14	35	5	0.88	103.6
15	45	3.5	0.88	96.1

$$\eta = \beta_0 + \sum_{j=1}^k \beta_j x_j + \sum_{j=1}^k \beta_{jj} x_j^2 + \sum_i \sum_{<j=2}^k \beta_{ij} x_i x_j + \dots + e_i \tag{2}$$

In this equation, η is the predicted response, x_i and x_j are the independent factors, β_0 is the constant coefficient, β_j , β_{jj} , and β_{ij} are the coefficients for linear, quadratic, and interaction effects and e_i is the error. Degree of freedom (df) is a scale of information that could be gained distinctively. The concept of df could be expanded to experiments. The coefficients of determination, R^2 and R^2_{adj} were used to imply the polynomial fitness quality. The analysis of variance (ANOVA) was also carried out in order to statistically analyze the results. It evaluates the model and its parameters, and also determines the individual and interactive influences of parameters on the response using the coefficients in Eq. (2). F -value, p -value, R^2 , and lack of fit were used in order to investigate how well the suggested model fits the experimental data [35–37]. Model terms were selected or rejected based on the probability value with 95% confidence level.

Table 2
Experimental range and levels of independent process variables

Independent variable (unit)	Low experimental value	High experimental value	Low coded value	High coded value
Temperature (°C)	25	45	–1	+1
TMP (bar)	2	5	–1	+1
CFV (m/s)	0.59	0.88	–1	+1

9. Results and discussion

9.1. Membrane characterization

Separation performance of the synthesized γ - Al_2O_3 active layer was evaluated via milk concentration. As shown in Table 4, the permeation results exhibited that permeate fluxes of water and milk after two times of coating extremely decrease, but turbidity slightly reduces. Hence, twice coating was considered as the optimum coating number.

Fig. 2 shows the XRD pattern of γ - Al_2O_3 layer after calcination at 550°C for 3 h. At this calcination temperature, the visible diffraction peaks corresponding to the major diffraction peaks of γ - Al_2O_3 at $2\theta = 45.38^\circ$ and 66.68° can be observed [2]. As seen, the sample consists of a single phase of well-crystalline γ - Al_2O_3 and no extra peaks of impurities are present. The α - Al_2O_3 support layer as macroporous layer was coated with a less porous γ - Al_2O_3 thin layer as active layer. The macroporous support layer was not suitable for oily wastewater treatment because significant amount of oil could pass through it. Thus, the active layer was required to increase its efficiency. The active layer had smaller pores and this prevented the oil permeation. Fig. 3 shows cross section SEM image of the support with its active layer. As observed, the thin active γ - Al_2O_3 layer is uniformly coated over the α - Al_2O_3 support. The SEM image confirms the successful coating of the support by the γ - Al_2O_3 layer. It is also observed that the coated active layer exhibits good uniformity and adhesiveness to the support and this is mostly because the both layers are made of alumina. As observed, thickness of the active γ - Al_2O_3 layer is approximately 4 μm . It is also observed that the γ - Al_2O_3 layer formed over the support surface possesses finer mesh compared with the support structure which can be due to the lower calcination temperature of γ - Al_2O_3 (550°C) compared with that of α - Al_2O_3 (1,400°C). The average pore size of γ - Al_2O_3 top layer was determined by BET analysis. It showed that average pore size and specific surface area of the γ - Al_2O_3 layer are 20.3 nm and 2.1 m^2/g , respectively.

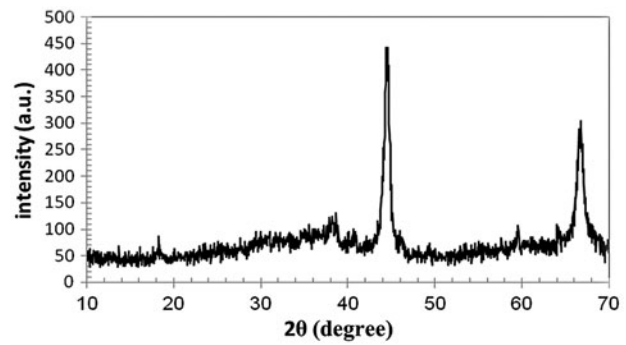


Fig. 2. XRD pattern of the γ - Al_2O_3 layer at 550°C.

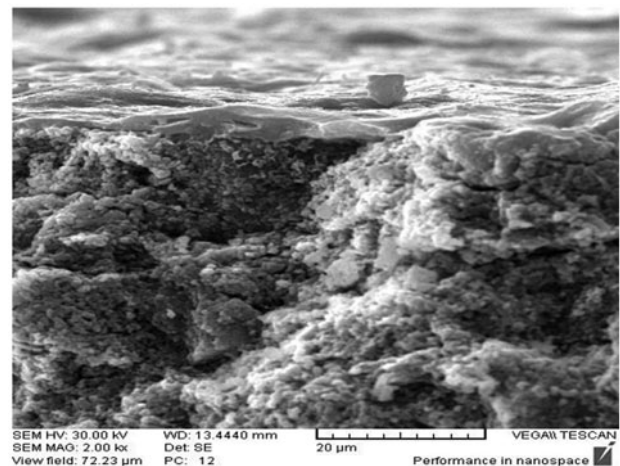


Fig. 3. Cross section SEM image of the double-layer γ - Al_2O_3 coated α - Al_2O_3 macroporous support.

9.2. Design of experiments using BBD

The experiments were verified using statistical analysis and a quadratic model was selected, as suggested by the software. The regression model equation for PF is shown as follows in terms of uncoded factors:

$$\begin{aligned} \text{PF} = & -235.38954 + 51.31481 \times \text{TMP} + 5.00333 \times T \\ & + 396.31391 \times \text{CFV} - 5.59259 \times \text{TMP}^2 \\ & - 0.064833 \times T^2 - 286.95997 \times \text{CFV}^2 \end{aligned} \quad (3)$$

Table 4
Effect of coating number on milk concentration

Coating number	Water flux ($\text{kg}/\text{m}^2 \text{ h}$)	Milk flux ($\text{kg}/\text{m}^2 \text{ h}$)	NTU
1	242.3	155.7	19.07
2	211.6	125.3	10.69
3	146.4	66.6	5.63

The values of the response determined by means of the regression equation using the model, Eq. (3), were compared with the obtained experimental data for each specific experiment as presented in from Table 3. The results are presented in Fig. 4. As observed, the model well predicts of the experimental data. Therefore, based on the statistical tests and the predictions results, the model can be accurately considered for UF simulation and optimization.

The ANOVA for the second-order polynomial equation is reported in Table 5. F -value represents noise and implied that the quadratic model can describe the experiments. Each term in the model was also tested for significance, p -value smaller than 0.05 implies that the corresponding model term is significant. The value greater than 0.1 indicates that the model terms are not significant. The linear and quadratic coefficients were found to be more significant than the interacting coefficients. ANOVA study suggested that TMP ($p < 0.0001$, $F = 19397.61$) has the most significant effect on PF followed by TMP^2 ($p < 0.0001$, $F = 4285.637$), T ($p < 0.0001$, $F = 1254.516$), T^2 ($p < 0.0001$, $F = 1132.54$), CFV^2 ($p < 0.0001$, $F = 973.8265$), and CFV ($p < 0.0001$, $F = 796.1006$). There is no interaction between parameters since the p -values for all the interacting coefficients are high. Therefore, they have no effects on the response and do not considered in Eq. (3). This is due to the fact that TMP is the most significant parameters on PF, therefore by increasing TMP PF increases significantly, and as the setup operated in batch mode by increasing PF more water passes through the membrane and this causes the feed concentration in the feed tank [38].

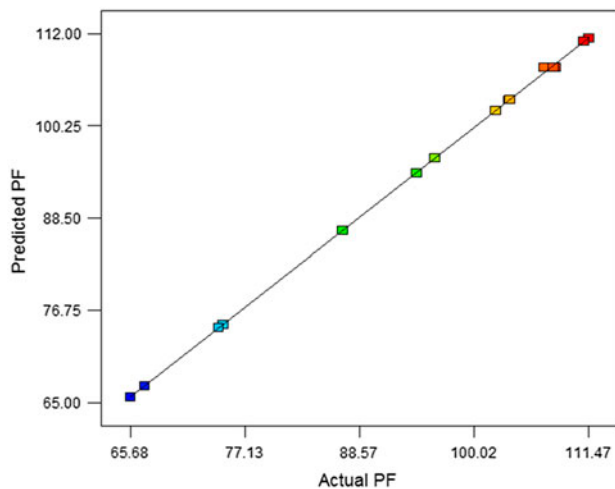


Fig. 4. Scatter diagram of predicted PF ($\text{kg}/\text{m}^2 \text{ h}$) vs. experimental PF ($\text{kg}/\text{m}^2 \text{ h}$).

Moreover, the lack of fit of 1.0000 shows that there is no relative to pure error. Predicted R^2 (R^2_{pre}) is a calculation of variation amount around the mean represented by the model. However, a large value of R^2_{pre} can mislead if the model contains additional terms. Adding factors to the model always increases R^2_{pre} whether the added parameters are significant or not. As factors are added to the model, the adjusted R^2 (R^2_{adj}) value does not increase. In fact, large differences between R^2_{pre} and R^2_{adj} express that non-significant terms are involved in the model. The R^2_{adj} and the R^2_{pre} should be within about 0.20 of each other, to be in acceptable agreement. If they are not, there may have a difficulty with either the data or the model. In this case, the R^2_{pre} and the R^2_{adj} are 0.9996 and 0.9995, respectively, and they are in acceptable agreement with each other. Adequate precision is signal-to-noise ratio (S/N), in other words a measure of the range in predicted response relative to its associated error. Its desired value is 4 or more [39,40]. The ratio of 151.290 indicates an adequate signal. The coefficient of variation for this model is the error expressed as a percentage of the mean.

9.3. Effects of operating conditions

Effects of the UF operating parameters on PF are plotted and contour plots in order to visualize the individual and the interactive effects of the independent variables are presented. As shown in Fig. 5, PF increases with increasing TMP. However, at high TMP, PF is nearly constant. This can be due to compression of the cake/gel layer formed on the membrane surface at high pressure. According to the Darcy's law, increasing TMP increases PF. However, fouling restricts this fundamental law. Increasing TMP makes the sediments more compact on the membrane surface and this blocks the membrane pores. Thus, at an optimum TMP, PF is high, while tendency to cake/gel layer formation is low [41,42]. The results show that TMP of 5 bar can be considered as the best operating TMP because at higher TMP, the cake/gel layer becomes denser and permeation do not increase any more.

Temperature exhibits double effects on PF; increasing temperature increases osmotic pressure, and this slightly decreases PF [41,43]. From another point of view, since permeate is mainly gas oil, its viscosity dramatically decreases with increasing temperature, and as a result, this increases the solvent and the solutes permeabilities (diffusivities) [26,44]. As shown in Fig. 5, increasing temperature up to 35°C increases PF because the viscosity effect is more significant than the osmotic pressure effect, however, further

Table 5
ANOVA results of the quadratic model for PF via UF process

Source	Sum of squares	df	Mean square	F-value	p-value Prob. > F	Remark	
Model	3,728.77	9	414.3078	3,016.25	<0.0001	Significant	
A-T	172.3186	1	172.3186	1,254.516	<0.0001		
B-TMP	2,664.428	1	2,664.428	19,397.61	<0.0001		
C-CFV	109.3513	1	109.3513	796.1006	<0.0001		
AB	0	1	0	0	1.0000		
AC	0	1	0	0	1.0000		
BC	0	1	0	0	1.0000		
A ²	155.5641	1	155.5641	1,132.54	<0.0001		
B ²	588.669	1	588.669	4,285.637	<0.0001		
C ²	133.7634	1	133.7634	973.8265	<0.0001		
Residual	0.686793	5	0.137359				Not significant
lack of fit	0	3	0	0	1.0000		
Pure error	0.686793	2	0.343396				
Corr. total	3,729.457	14					
Std. dev.	0.37		R ²	0.9998			
Mean	94.29		Adj R ²	0.9995			
C.V.%	0.39		Pred R ²	0.9996			
Press	1.55		Adeq precision	151.290			

increasing temperature has negative effect on PF. The osmotic pressure effect slightly enhances and the viscosity effect diminishes at higher temperature. Based on the results, temperature of 35°C can be recommended to achieve high PF at low operational costs.

Increasing CFV increases mass transfer coefficient in the concentration boundary layer and enhances turbulence over the membrane surface. This can reduce aggregation of the sediments in the cake/gel layer, and as a result, the aggregated materials on the membrane surface diffuse back to the bulk solution, so the concentration polarization effects diminish. This leads to increase the effective pressure difference consequently, and thus, PF increases [45,46]. In Fig. 5, effects of CFV on PF are presented. As observed, PF increases with increasing CFV till 0.735 m/s. Further increasing CFV decreases the effective pressure difference. Thus PF decreases. Considering that higher CFV leads to more power consumption for pumping, so

the choice of very high CFVs is not economically feasible. Therefore, the optimum CFV can be considered as 0.735 m/s.

9.4. Performance of the UF membranes at best operating conditions

Optimum values of the factors (process parameters) for the maximum response values were determined, as shown in Table 6. An experiment at the optimum operating conditions was performed to confirm the model suitability for predicting the maximum response value. The obtained experimental value and its associated predicted value from the experiment were compared for further residual and percentage error analysis. The percentage error between experimental and predicted values of the response was calculated as follows:

Table 6
Optimum values of the factors (process parameters) for the maximum response results

Factors	Optimum value (units)
PF	113.3 (kg/m ² h)
T	35 (°C)
TMP	5 (bar)
CFV	0.735 (m/s)

Table 7
Predicted and experimental values for the responses at the optimum condition

Response	PF (kg/m ² h)
Predicted	113.3
Experimental	112.7
Residual	0.6
% Error	0.53

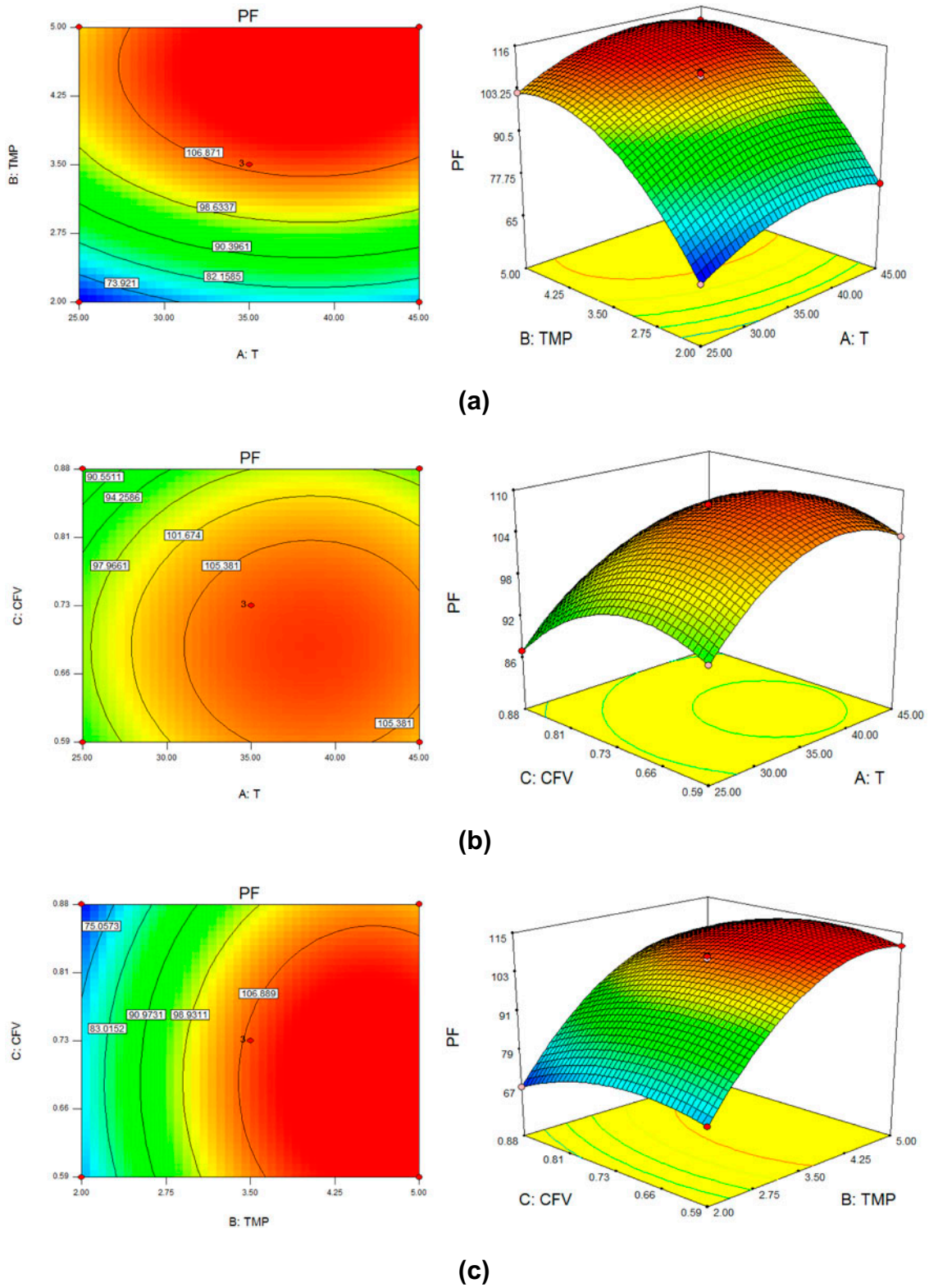


Fig. 5. Effect of TMP, T , and CFV on performance of the $\gamma\text{-Al}_2\text{O}_3$ membrane: (a) $\text{CFV} = 0.735 \text{ m/s}$, (b) $\text{TMP} = 3.5 \text{ bar}$, and (c) $T = 35^\circ\text{C}$

Table 8
Performance of different membrane

Parameter	γ -Al ₂ O ₃ (This work)		Mullite [46]		PVDF [47]		Standard ^a [47]
	Feed	Permeate	Feed	Permeate	Feed	Permeate	
COD	416	125	510	44	555	400	400
TSS	210	30	60	Trace	213	100	100
OGC	69	11	1000	63	17	10	10

^aNational primary discharged standard (P.U. (A) 434, Standard B, December 10, 2011).

$$\% \text{ Error} = \frac{\text{Residual}}{\text{Experimental value}} \times 100 \quad (4)$$

where the residual can be determined from the difference between experimental and predicted values. The results presented in Table 7 show that the percentage error implied by the developed empirical model is considerably small for the response. The maximum value of 3% for the percentage error between the experimental and the predicted values is well and suggests that the model is acceptable at least within 97% of the prediction interval [40]. The good agreement between the experimental and the predicted results verifies validity of the model and confirms existence of the optimal point.

9.5. Wastewater treatment experiments

Wastewater treatment experiments using the effluent from feed were conducted at T of 35°C, TMP of 5 bar and CFV of 0.735 m/s. The UF process was performed for 8 h continually. Fig. 6 shows PF as a function of filtration time. At the beginning, it decreases significantly and then decreases slightly until it becomes almost constant. The initial significant decline

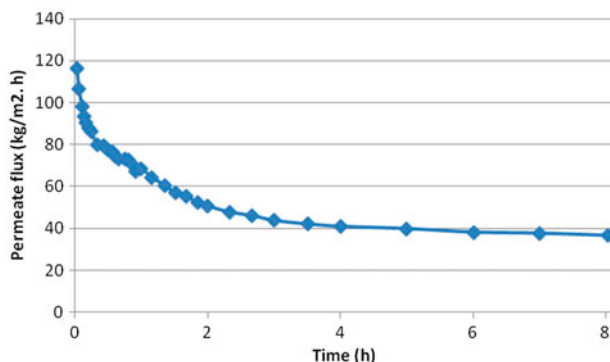


Fig. 6. PF decline for the γ -Al₂O₃ membrane (TMP = 5 bar, T = 35°C, and CFV = 0.735 m/s).

can be attributed to formation of the concentration polarization layer, while the further gradual decline can be attributed to the membrane fouling [13,17]. Formation of a cake/gel layer over the membrane surface is responsible for the decline.

9.6. Water quality analysis

In order to investigate the UF performance, the feed and the permeate samples were analyzed. The results are presented in Table 1. As observed, the membrane is able to treat the wastewater and the permeate can be qualified for agriculture expenses (according to the environmental standards). As shown in Table 8, performance of the γ -Al₂O₃ membrane was compared with those of other membranes [43,46,47] and national primary discharged standard [47]. In comparison to others, results showed that the synthesized γ -Al₂O₃ UF membrane exhibits acceptable performance for the wastewater treatment [47,48].

10. Conclusion

In this work, RSM by BBD was used to examine the effects of three operating parameters, T = 25–45°C, TMP = 2–5 bar, and CFV = 0.59–0.88 m/s, on real oily wastewater treatment process using the synthesized γ -Al₂O₃ ceramic UF membrane. The results showed that RSM is a suitable approach to optimize the operating conditions for achieving the optimum oily wastewater treatment via UF process. It was shown that the R^2_{pre} value of 0.9996 is in acceptable agreement with the R^2_{adj} value of 0.9995. The model indicated that T of 35°C, TMP of 5 bar, and CFV of 0.735 m/s are optimum conditions for obtaining the maximum PF.

The results showed that the synthesized membrane is able to effectively separate oil from the oily wastewater via cross-flow UF and the oil content in the permeate does almost meet the discharge standard of 10 mg/l. Additionally, this suggests that the UF operational unit can be followed by another operational unit, e.g. NF or RO in order to absolutely meet the

national primary discharge standard of 10 mg/l for OGC based on discharged standard. According to the obtained results, it can be concluded that UF using economically alumina ceramic membrane can be employed as an advanced method for pretreatment of the oily wastewater. It is prior to membrane filtration, since it is necessary to maintain a high and steady flux through the membrane to obtain a good process performance and to extend membrane life.

Nomenclature

PF	—	permeate flux (kg/m ² h)
V	—	volume of permeate collected (m ³)
A	—	effective membrane area (m ²)
t	—	time (h)
μ	—	feed viscosity (Pa s)
ΣR	—	summation of resistances in the direction of permeation
PF _{wi}	—	pure water flux (kg/m ² h)
PF _{ww}	—	the pure water flux through the fouled membrane after filtration (kg/m ² h)
η	—	predicted response
x _i , x _j	—	the independent factors
β ₀	—	constant coefficient
β _j	—	coefficient for linear effect
β _{jj}	—	coefficient for quadratic effect
β _{ij}	—	coefficient for interaction effect
e _i	—	error

References

- [1] U. Daiminger, W. Nitsch, P. Plucinski, S. Hoffmann, Novel techniques for oil/water separation, *J. Membr. Sci.* 99 (1995) 197–203.
- [2] A. Hong, A.G. Fane, R. Burford, Factors affecting membrane coalescence of stable oil-in-water emulsions, *J. Membr. Sci.* 222 (2003) 19–39.
- [3] A. Lobo, Á. Cambiella, J.M. Benito, C. Pazos, J. Coca, Ultrafiltration of oil-in-water emulsions with ceramic membranes: Influence of pH and crossflow velocity, *J. Membr. Sci.* 278 (2006) 328–334.
- [4] J. Brinck, A.S. Jönsson, B. Jönsson, J. Lindau, Influence of pH on the adsorptive fouling of ultrafiltration membranes by fatty acid, *J. Membr. Sci.* 164 (2000) 187–194.
- [5] S. Elmaleh, N. Ghaffor, Cross-flow ultrafiltration of hydrocarbon and biological solid mixed suspensions, *J. Membr. Sci.* 118 (1996) 111–120.
- [6] J. Zhong, X. Sun, C. Wang, Treatment of oily wastewater produced from refinery processes using flocculation and ceramic membrane filtration, *Sep. Purif. Technol.* 32 (2003) 93–98.
- [7] H. Zhu, X. Wen, X. Huang, Characterization of membrane fouling in a microfiltration ceramic membrane system treating secondary effluent, *Desalination* 284 (2012) 324–331.
- [8] S. Lee, Y. Aurelle, H. Roques, Concentration polarization, membrane fouling and cleaning in ultrafiltration of soluble oil, *J. Membr. Sci.* 19 (1984) 23–38.
- [9] P. Wang, N. Xu, J. Shi, A pilot study of the treatment of waste rolling emulsion using zirconia microfiltration membranes, *J. Membr. Sci.* 173 (2000) 159–166.
- [10] A. Lobo, A. Cambiella, J.M. Benito, C. Pazos, J. Coca, Effect of a previous coagulation stage on the ultrafiltration of a metalworking emulsion using ceramic membranes, *Desalination* 200 (2006) 330–332.
- [11] H. Zhang, Z. Zhong, W. Xing, Application of ceramic membranes in the treatment of oilfield-produced water: Effects of polyacrylamide and inorganic salts, *Desalination* 309 (2013) 84–90.
- [12] N. Nabi, P. Aimar, M. Meireles, Ultrafiltration of an olive oil emulsion stabilized by an anionic surfactant, *J. Membr. Sci.* 166 (2000) 177–188.
- [13] Y.S. Li, L. Yan, C.B. Xiang, L.J. Hong, Treatment of oily wastewater by organic–inorganic composite tubular ultrafiltration (UF) membranes, *Desalination* 196 (2006) 76–83.
- [14] S.H.D. Silalahi, T. Leiknes, Cleaning strategies in ceramic microfiltration membranes fouled by oil and particulate matter in produced water, *Desalination* 236 (2009) 160–169.
- [15] M. Bodzek, K. Konieczny, The use of ultrafiltration membranes made of various polymers in the treatment of oil-emulsion wastewaters, *Waste Manage.* 12 (1992) 75–84.
- [16] T. Mohammadi, M. Kazemimoghadam, M. Saadabadi, Modeling of membrane fouling and flux decline in reverse osmosis during separation of oil in water emulsions, *Desalination* 157 (2003) 369–375.
- [17] X. Hu, E. Bekassy-Molnar, A. Koris, Study of modelling transmembrane pressure and gel resistance in ultrafiltration of oily emulsion, *Desalination* 163 (2004) 355–360.
- [18] M. Karhu, T. Kuokkanen, J. Rämö, M. Mikola, J. Tanskanen, Performance of a commercial industrial-scale UF-based process for treatment of oily wastewaters, *J. Environ. Manage.* 128 (2013) 413–420.
- [19] D. Vasanth, G. Pugazhenthii, R. Uppaluri, Fabrication and properties of low cost ceramic microfiltration membranes for separation of oil and bacteria from its solution, *J. Membr. Sci.* 379 (2011) 154–163.
- [20] R. Scheibler, E.R.F. Santos, A.S. Barbosa, M.G.F. Rodrigues, Performance of zeolite membrane (ZSM-5/γ-Alumina) in the oil/water separation process, *Desalin. Water Treat.* 56 (2015) 3561–3567.
- [21] Q. Chang, X. Wang, Y. Wang, X. Zhang, S. Cerneaux, J.-e. Zhou, Effect of hydrophilic modification with nano-titania and operation modes on the oil–water separation performance of microfiltration membrane, *Desalin. Water Treat.* 57 (2016) 4788–4795.
- [22] S. Barredo-Damas, M.I. Alcaina-Miranda, M.I. Iborra-Clar, J.A. Mendoza-Roca, M. Gemma, Effect of pH and MWCO on textile effluents ultrafiltration by tubular ceramic membranes, *Desalin. Water Treat.* 27 (2011) 81–89.
- [23] D. Allende, D. Pando, M. Matos, C.E. Carleos, C. Pazos, J.M. Benito, Optimization of a membrane hybrid process for oil-in-water emulsions treatment using Taguchi experimental design, *Desalin. Water Treat.* 57 (2015) 4832–4841.

- [24] K. Majewska-Nowak, J. Kawiecka-Skowron, Ceramic membrane behaviour in anionic dye removal by ultrafiltration, *Desalin. Water Treat.* 34 (2011) 367–373.
- [25] W.C. Wong, L.T.Y. Au, C.T. Ariso, K.L. Yeung, Effects of synthesis parameters on the zeolite membrane growth, *J. Membr. Sci.* 191 (2001) 143–163.
- [26] M. Kazemimoghadam, T. Mohammadi, Chemical cleaning of ultrafiltration membranes in the milk industry, *Desalination* 204 (2007) 213–218.
- [27] X. Fan, Y. Tao, L. Wang, X. Zhang, Y. Lei, Z. Wang, H. Noguchi, Performance of an integrated process combining ozonation with ceramic membrane ultrafiltration for advanced treatment of drinking water, *Desalination* 335 (2014) 47–54.
- [28] F.L. Hua, Y.F. Tsang, Y.J. Wang, S.Y. Chan, H. Chua, S.N. Sin, Performance study of ceramic microfiltration membrane for oily wastewater treatment, *Chem. Eng. J.* 128 (2007) 169–175.
- [29] J. Lindau, A.S. Jönsson, Cleaning of ultrafiltration membranes after treatment of oily waste water, *J. Membr. Sci.* 87 (1994) 71–78.
- [30] S.K.S. Al-Obeidani, H. Al-Hinai, M.F.A. Goosen, S. Sablani, Y. Taniguchi, H. Okamura, Chemical cleaning of oil contaminated polyethylene hollow fiber microfiltration membranes, *J. Membr. Sci.* 307 (2008) 299–308.
- [31] B. Yoldas, Alumina gels that form porous transparent Al_2O_3 , *J. Mater. Sci.* 10 (1975) 1856–1860.
- [32] L.S. Clesceri, A.E. Greenberg, A.D. Eaton, *Standard Methods for the Examination of Water and Wastewater*, twentieth ed., APHA, Washington, DC, 1998.
- [33] M. Padaki, R. Surya Murali, M.S. Abdullah, N. Misdan, A. Moslehyani, M.A. Kassim, N. Hilal, A.F. Ismail, Membrane technology enhancement in oil–water separation. A review, *Desalination* 357 (2015) 197–207.
- [34] C. Wu, A. Li, L. Li, L. Zhang, H. Wang, X. Qi, Q. Zhang, Treatment of oily water by a poly(vinyl alcohol) ultrafiltration membrane, *Desalination* 225 (2008) 312–321.
- [35] H. Ceylan, S. Kubilay, N. Aktas, N. Sahiner, An approach for prediction of optimum reaction conditions for laccase-catalyzed bio-transformation of 1-naphthol by response surface methodology (RSM), *Bioresour. Technol.* 99 (2008) 2025–2031.
- [36] G. Voneiff, S. Sadeghi, P. Bastian, B. Wolters, J. Jochen, B. Chow, K. Chow, M. Gatens, Probabilistic Forecasting of Horizontal Well Performance in Unconventional Reservoirs Using Publicly-Available Completion Data, in: SPE Unconventional Resources Conference, Sci. Petro. Eng, The Woodlands, Texas, USA, 2014.
- [37] G. Voneiff, S. Sadeghi, P. Bastian, B. Wolters, J. Jochen, B. Chow, K. Chow, M. Gatens, A Well Performance Model Based on Multivariate Analysis of Completion and Production Data from Horizontal Wells in the Montney Formation in British Columbia, in: Sci. Petro. Eng, The Woodlands, Texas, USA, 2014.
- [38] X. Yuan, J. Liu, G. Zeng, J. Shi, J. Tong, G. Huang, Optimization of conversion of waste rapeseed oil with high FFA to biodiesel using response surface methodology, *Renewable Energy* 33 (2008) 1678–1684.
- [39] N. Aghamohammadi, H.B.A. Aziz, M.H. Isa, A.A. Zinatizadeh, Powdered activated carbon augmented activated sludge process for treatment of semi-aerobic landfill leachate using response surface methodology, *Bioresour. Technol.* 98 (2007) 3570–3578.
- [40] A.W. Zularisam, A.F. Ismail, M.R. Salim, M. Sakinah, T. Matsuura, Application of coagulation–ultrafiltration hybrid process for drinking water treatment: Optimization of operating conditions using experimental design, *Sep. Purif. Technol.* 65 (2009) 193–210.
- [41] T. Mohammadi, A. Esmaelifar, Wastewater treatment of a vegetable oil factory by a hybrid ultrafiltration-activated carbon process, *J. Membr. Sci.* 254 (2005) 129–137.
- [42] X.-H. Zhen, S.-L. Yu, B.-F. Wang, H.-F. Zheng, Flux enhancement during ultrafiltration of produced water using turbulence promoter, *J. Environ. Sci.* 18 (2006) 1077–1081.
- [43] A. Salahi, T. Mohammadi, A. Rahmat Pour, F. Rekabdar, Oily wastewater treatment using ultrafiltration, *Desalin. Water Treat.* 6 (2009) 289–298.
- [44] C.B. Spricigo, A. Bolzan, R.A.F. Machado, L.H.C. Carlson, J.C.C. Petrus, Separation of nutmeg essential oil and dense CO_2 with a cellulose acetate reverse osmosis membrane, *J. Membr. Sci.* 188 (2001) 173–179.
- [45] M.C.V. Vela, S.Á. Blanco, J.L. García, E.B. Rodríguez, Analysis of membrane pore blocking models applied to the ultrafiltration of PEG, *Sep. Purif. Technol.* 62 (2008) 489–498.
- [46] M. Abbasi, A. Salahi, M. Mirfendereski, T. Mohammadi, A. Pak, Dimensional analysis of permeation flux for microfiltration of oily wastewaters using mullite ceramic membranes, *Desalination* 252 (2010) 113–119.
- [47] E. Yuliwati, A.F. Ismail, T. Matsuura, M.A. Kassim, M.S. Abdullah, Effect of modified PVDF hollow fiber submerged ultrafiltration membrane for refinery wastewater treatment, *Desalination* 283 (2011) 214–220.
- [48] A. Salahi, M. Abbasi, T. Mohammadi, Permeate flux decline during UF of oily wastewater: Experimental and modeling, *Desalination* 251 (2010) 153–160.